Stem Cell Research (2013) 10, 288–300

Available online at www.sciencedirect.com

SciVerse ScienceDirect

www.elsevier.com/locate/scr

Therapeutic potential of human-induced pluripotent stem cell-derived endothelial cells in a bleomycin-induced scleroderma mouse model

Manizheh Azhdari [a,b], Mohamadreza Baghaban-Eslaminejad [a], Hossein Baharvand [a,b,c,*], Nasser Aghdami [a,c,**]

[a] Department of Stem Cells and Developmental Biology, Cell Science Research Center, Royan Institute for Stem Cell Biology and Technology, ACECR, Tehran, Iran
[b] Department of Developmental Biology, University of Science and Culture, ACECR, Tehran, Iran
[c] Department of Regenerative Medicine, Cell Science Research Center, Royan Institute for Stem Cell Biology and Technology, ACECR, Tehran, Iran

Received 27 July 2012; received in revised form 15 November 2012; accepted 12 December 2012

Abstract Vascular injury and destruction of endothelial cells (ECs) are the early events in scleroderma (SSc) patients. This study aims to investigate the therapeutic potential of human-induced pluripotent stem cell-derived ECs (hiPSC-ECs) to treat SSc. We have assessed the functional differentiation of hiPSC-ECs and compared them with human embryonic stem cell-derived ECs (hESC-ECs) by a variety of in vitro experimental approaches. Additionally, we evaluated the therapeutic potential of hiPSC-ECs in a bleomycin-induced SSc mouse model. Our results demonstrated that hiPSC-ECs and hESC-ECs showed similar maximum expressions of FLK1 (early EC marker) at day five during differentiation. After sorting and culturing, the FLK1-positive cells exhibited spindle and subsequent endothelial cobblestone morphology in EGM2 medium. The hESC-ECs and hiPSC-ECs also expressed late EC markers CD31 (68% and 75%), CD144 (50% and 61%), CD146 (46% and 61%), and DiI-labeled acetylated low-density lipoprotein (DiI-ac-LDL) uptake (55% and 63%), respectively. They additionally formed capillary-like structures on Matrigel. Analyses of the transplantation of sorted CD31-positive hiPSC-ECs into the bleomycin-induced SSc mouse model demonstrated that these cells participate in recovery of the damaged vessels. There was a reduction in collagen content; the number of total and degranulated mast cells returned to their normal state, and bleomycin-induced wounds as well as skin fibrosis improved four weeks after transplantation of hiPSC-ECs. Our findings have shown that the differentiation process from hESCs and hiPSCs to vascular cell components is similar. Additionally, this is the first study to determine the therapeutic potential of vascular cells from hiPSCs in the treatment of an SSc model. In the future, with further validation, these may be used as an appropriate source for the treatment of SSc patients.
© 2012 Elsevier B.V. All rights reserved.

* Correspondence to: H. Baharvand, Department of Stem Cells and Developmental Biology, Cell Science Research Center, Royan Institute for Stem Cell Biology and Technology, ACECR, Tehran, Iran. Fax: +98 21 22310406.
** Correspondence to: N. Aghdami, Department of Stem Cells and Developmental Biology, Cell Science Research Center, Royan Institute for Stem Cell Biology and Technology, ACECR, Tehran, Iran.
E-mail addresses: Baharvand@RoyanInstitute.org (H. Baharvand), Nasser.Aghdami@RoyanInstitute.org (N. Aghdami).

1873-5061/$ - see front matter © 2012 Elsevier B.V. All rights reserved.
http://dx.doi.org/10.1016/j.scr.2012.12.004

Introduction

Scleroderma (systemic sclerosis, SSc) is a connective tissue disease characterized by vascular injury, the excessive accumulation of extracellular matrix (ECM) proteins in the skin and various internal organs, and immunological abnormalities (Yamamoto, 2009). SSc is resistant to all types of treatments (Yamamoto, 2009). Endothelial cells (ECs) are affected in the early stages of SSc (Gabrielli et al., 2009; Kahaleh, 2008). In early lesions there are changes of the endothelial phenotype or EC apoptosis in the absence of EC proliferation or precursor differentiation (Gabrielli et al., 2009; Kahaleh, 2008). It has been reported that mesenchymal stem cells (MSCs) and endothelial progenitor cells (EPCs) from SSc patients show abnormalities in differentiation to ECs (Cipriani et al., 2007; Trojanowska, 2010). Recently, clinical improvement in patients with SSc has been demonstrated following administration of high dose immunosuppressive therapy and autologous hematopoietic cell transplantation (Fleming et al., 2008). Additionally, it has been demonstrated that isolated EPCs from normal peripheral blood participate and increase the formation of new blood vessels (Asahara et al., 1999; Isner et al., 2001). However, isolation of EPCs from adults has limited replicative capacity. In elderly patients with cardiovascular risk factors, EPCs are few in number and dysfunctional (Heeschen et al., 2004; Hill et al., 2003; Vasa et al., 2001). The discovery of human embryonic stem (hESCs) (Thomson et al., 1998) and human-induced pluripotent stem cells (hiPSCs) (Takahashi et al., 2007; Yu et al., 2007), due to their capacities for self-renewal and pluripotency, have provided fascinating possibilities and hopes for curing diseases that have poor prognoses. Until now, several reports have described the differentiation and functionality of ECs derived from murine (Kim and von Recum, 2009; Li et al., 2007; Sone et al., 2003; Yamashita et al., 2000), primate (Kaufman et al., 2004; Sone et al., 2003), and human (Levenberg et al., 2002; Li et al., 2011) ESCs or iPSCs (Li et al., 2011; Rufaihah et al., 2011). The beneficial influences of hESC-derived ECs (hESC-ECs) in the setting of myocardial or limb ischemia has been reported (James et al., 2010; Kane et al., 2010; Levenberg et al., 2002, 2010; Li et al., 2009; Nourse et al., 2010; Rufaihah et al., 2010; Sone et al., 2007). Transplantation of hiPSC-ECs also enhanced capillary density and improved reperfusion in a limb ischemia mouse model (Rufaihah et al., 2011). However, no study has yet reported the therapeutic potential of hESC-ECs or hiPSC-ECs in the treatment of damaged vessels that result from SSc.

Therefore, in this report, initially we induced hESCs and hiPSCs into mesodermal FLK1-positive cells. Subsequently, these positive cells were sorted and differentiated into ECs. Considering the characterization of these differentiated cells and comparing their functionality, we have concluded that hiPSCs can efficiently differentiate into ECs in a manner similar to hESCs. Finally, we have evaluated the therapeutic potential of transplanted hiPSC-ECs into a bleomycin-induced SSc mouse model and investigated the synthesis of TGF-β1, total and degranulated mast cell numbers, and collagen content alternation.

Materials and methods

Antibodies

Monoclonal antibodies for human FLK1 (1:100, GR8507-2) were purchased from Abcam. Monoclonal antibodies for human CD31 (1:200, 555444), CD144 (1:200, 555661), CD146 (1:200, 550314), vWF (1:200, 555849), and CD45 (1:200, 345808) for immunostaining and flow cytometry were obtained from Beckton Dickenson (BD). Secondary murine polyclonal antibodies IgG1-FITC (1:200, 04611) and IgG1-PE (1:200, 340270) were purchased from BD.

hESCs and hiPSCs culture and EC differentiation

hESCs (Royan H5, 46XX) and hiPSCs (hiPSC1, 46XY, derived from a healthy 40-year-old Iranian male) were obtained from the Stem Cell Bank at Royan Institute (Baharvand et al., 2006; Totonchi et al., 2010) and cultured feeder-free on Matrigel (1:30, Sigma-Aldrich, E1270)-coated cell culture dishes in DMEM-F12 (Gibco-Invitrogen, 21331-020, USA) supplemented with 10% knockout serum replacement (KOSR, Gibco-Invitrogen, 10828-028), 2 mM L-glutamine (Gibco-Invitrogen, 25030-024), 0.1 mM 2-mercaptoethanol (Sigma-Aldrich, M7522, USA), 1% nonessential amino acids (NEAAs, Gibco-Invitrogen, 11140-035), 100 IU/ml penicillin, 100 mg/ml streptomycin (Gibco-Invitrogen, 15070-063), insulin-transferrin-selenite (ITS, Gibco-Invitrogen, 41400-045), and 100 ng/ml basic fibroblast growth factor (bFGF, Royan Institute). hESCs and hiPSCs were induced to differentiate as described previously (Levenberg et al., 2010). Briefly, $5–6\times10^4$ hESCs or hiPSCs were cultured for six days on type-IV collagen-coated dishes (0.5 mg/ml, Sigma-Aldrich, C5533) in α-MEM medium (Gibco-Invitrogen, 22571) supplemented with 10% fetal bovine serum (FBS, Gibco-Invitrogen, 10270106), 1% NEAAs, and 1% penicillin/streptomycin. The cells were dissociated with collagenase (1 mg/ml, Gibco-Invitrogen, 17104-019) and dispase (2 mg/ml, Gibco-Invitrogen, 17105-041) for 10 min. FLK1-positive sorted cells were subcultured on collagen type I (8 μg/cm^2, Sigma-Aldrich, C3867) with EGM-2 medium (Lonza, CC-3162) until confluency.

Human umbilical vein endothelial cell isolation and culture

Umbilical cords from newborn infants were washed with phosphate buffered saline (PBS, Gibco-Invitrogen, 21600-069) to remove internal blood. Then, veins were filled with collagenase IV (0.1%, 1 mg/ml) and incubated at 37 °C for 10 min. After collecting the cell suspensions and centrifuging at 4 °C and 1500 rpm, cell pellets were cultured in M-199 medium (Gibco-Invitrogen, 31100-027) supplemented with 10% FBS, 1% NEAA, and 1% penicillin/streptomycin.

Flow cytometry and cell sorting

After induction of FLK1-positive cells on collagen IV and α-MEM medium, at differentiation day 5, cells were dissociated with trypsin/EDTA (Gibco-Invitrogen, 15400-054). Following neutralization with α-MEM supplemented with 10% FBS, cells were

washed in PBS that contained 2% FBS (FACS buffer). Subsequently, cells were allowed to incubate for 1 h at 4 °C with mouse IgG1 monoclonal anti-human FLK-1 and then washed with FACS buffer. Secondary polyclonal rat anti-mouse IgG1-PE or FITC was added and cells incubated for 1 h at 4 °C. After washing with FACS buffer, FLK1-positive cells were sorted by FACS Calibur (USA). This method was also used for sorting CD31-positive cells in EGM-2 medium. After differentiation of FLK1-positive cells into ECs in EGM-2 medium, the cells were dissociated using trypsin/EDTA after reaching confluency. Afterwards, cells were fixed with 4% paraformaldehyde (Sigma-Aldrich, P6148) and stained with monoclonal antibodies for CD31, CD144, CD146, FLK1, and CD45. Cells were washed twice with PBS before being subjected to flow cytometry analysis (FACS Aria, USA).

Immunostaining

Cells were fixed in 4% paraformaldehyde, blocked by 1% rat serum (Royan Institute), and incubated overnight with primary antibodies at 4 °C. Anti-mouse IgG antibodies conjugated with PE or FITC were used as secondary antibodies. Nuclei were stained with DAPI (1:1000 Sigma-Aldrich, D-8417). After each incubation, cells were washed twice with PBS. Stained cells were photographed with fluorescence microscopy (BX51; Olympus; Japan). To quantify the numbers of hESC-ECs and hiPSC-ECs, positively stained cells were counted in 12 randomly selected fields. Each experiment was repeated at least three times, with 3–4 slides each time, and approximately 2000 cells totally were counted.

Colony-forming assay

Endothelial cell colony-forming units (CFU-ECs) were cultured using the EndoCult Liquid Medium Kit (Stem Cell Technologies, 05901-2, Vancouver, BC, Canada) as per the manufacturer's protocol. FLK1-positive sorted cells were resuspended in complete EndoCult medium and seeded at $10–15\times10^3$ cells/well on fibronectin (Sigma-Aldrich, F-0635)-coated tissue culture plates. Cells were incubated at 37 °C and 5% CO_2 for 21 days. The cells were supplemented with new growth media four days after plating. At 7, 14, and 21 days after plating the numbers of CFU-ECs were counted in a minimum of three wells. A colony was defined as a central cluster of round cells with spindle-shaped cells that radiated from the periphery (Hill et al., 2003).

Uptake of acetylated low-density lipoprotein (DiI-ac-LDL)

Acetylated low-density lipoprotein (DiI-ac-LDL; Biomedical Technologies Inc., MA) was diluted to 10 μg/ml in complete growth medium and added to the cells and the mixture was allowed to incubate for 4 h at 37 °C. Then, we removed the medium and washed the cells with probe-free media. Cells were fixed with 4% paraformaldehyde. The nuclei were stained with 4, 6-diamidino-2-phenylindole (DPAI, 1:1000 Sigma-Aldrich, D-8417) and finally visualized with fluorescence microscopy.

Tube formation by ECs in vitro

ECs were cultured to form tubes in vitro as described previously (Balconi et al., 2000). Briefly, Matrigel matrix was diluted to 0.5–0.7 mg/ml in endothelial differentiation medium. ECs that were differentiated for five passages were trypsinized and replated at $3–5\times10^4$ cells in 300 μl of 0.5–0.7 mg/ml Matrigel onto each well of the 12-well plates. The Matrigel-cell suspension was polymerized for 2–4 h at 37 °C. Again, 300 μl of endothelial differentiation medium was added by semi-depletion to the dish and cells were incubated at 37 °C and 5% CO_2. The structures were photographed under phase contrast microscope (Olympus, IX71).

Scleroderma mouse model and hiPSC-EC transplantation

All animal care, surgical processes and post-operative euthanasia were undertaken in strict accordance with the approval of the Institutional Review Board and Institutional Ethical Committee at Royan Institute. All efforts were made to minimize the number of animals used. The SSc animal model was induced in six-week old female BALB/C mice (Pasteur Institute, Tehran, Iran) by daily subcutaneous injections of bleomycin (100 μg/ml, Merck, 46520202) for 4 weeks as previously described (Yamamoto, 2010). Additionally, cell-recipient mice were injected with cyclosporine solution (SandImmune; Novartis Pharmaceuticals, Switzerland) intraperitoneally at a dose of 20 mg/kg/24 h.

Then, hiPSC-ECs (1×10^6 cells in 100 μl of culture media; n=7–8 mice/group) were injected subcutaneously in three equidistant sites of the sclerotic skin. Control SSc mice were injected only with bleomycin (100 μg/ml) for 4 weeks. To study differentiated EC tracing, we labeled the cells with fluorescent DiI dye (Cell Tracker CM-DiI, Invitrogen Molecular Probes, 697948). Before transplantation, cells in the suspension were washed with PBS and incubated with DiI at a concentration of 2.5 μg/ml PBS for 5 min at 37 °C and 15 min at 4 °C. After two washing steps in PBS, the cells were resuspended in EGM-2 medium.

Histopathology and immunohistochemistry

The dorsal skin of the neck was removed after the final injection at one and four weeks post-transplantation. The skin pieces were fixed in 10% formalin solution and embedded in paraffin. Six micrometer-thick paraffin sections were prepared on poly L-lysine-coated slides. The sections were counterstained with Masson's trichrome (MT) stain, dehydrated, cleared, and mounted. Dermal thickness was measured after taking photographs under a light microscope of the MT stained sections and quantified by Image J software version 1.4. To evaluate the fate of labeled transplanted cells at 1 and 4 weeks post-transplantation, slides were stained with anti-vWF antibody. Briefly, sections were simultaneously blocked in serum and permeabilized with 0.2% Triton X-100 for 30 min at 37 °C. The primary antibody (1:200, mouse anti-human vWF) was diluted in blocking solution and sections were incubated overnight at room temperature. Secondary antibody (1:200, rat anti-mouse IgG-FITC) was applied for 1 h at 37 °C followed by washing with PBS. All washes consisted of

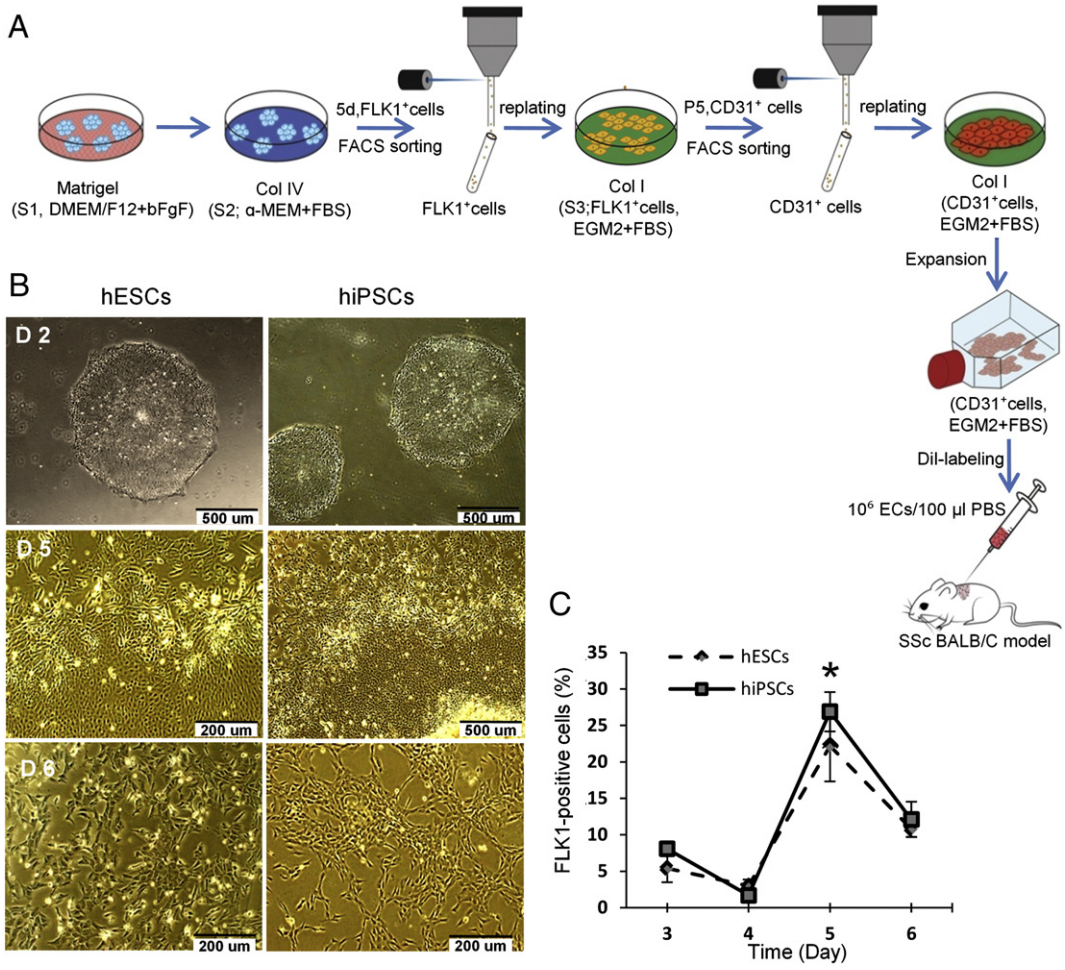


Figure 1 Differentiation of hESCs and hiPSCs into endothelial cells (ECs). (A) Schematic representation of the differentiation from hESCs and hiPSCs to endothelial cells (ECs) and transplantation into a scleroderma (SSc) mouse model. S: stage, D: day, P: passage, Col: collagen. (B) Phase-contrast images show similar EC differentiation and growth characteristics of hESCs and hiPSCs on collagen IV-coated dishes. (C) Flow cytometric analysis of hESCs and hiPSCs-derived FLK1-positive cells on collagen IV-coated dishes revealed maximum expression on day 5 during differentiation (*$P<0.05$).

two, 5 minute washes at room temperature using PBS. Nuclei were counterstained with DAPI and sections visualized using a fluorescence microscope (Olympus BX51; Japan). At each stage, control sections were incubated with blocking serum without antibody to confirm antibody specificity.

Mast cell number

Mast cells were identified by toluidine blue staining. Cells that contained metachromatic granules were counted in 12 random fields under light microscope power field magnifications of 4×,

Figure 2 Characterization of hESC- and hiPSC-derived FLK1-positive cells. (A) The purity of FLK1-positive cells from hESCs and hiPSCs increased after FACS. (B) CFU-EC colonies generated from hiPSC-FLK1-positive cells in EndoCult medium. Phase-contrast micrograph of a hiPSC-endothelial progenitor cell (hiPSC-EPC) colony defined by a central cluster of rounded cells that is surrounded by radiating thin and flat cells. The first colony was observed after seven days in culture. Similar colonies were observed in hESC-FLK1 (data not shown). CFU: colony-forming unit. (C) Quantification of CFU-ECs in hESC-ECs and hiPSC-ECs. (D) Sorted FLK1-positive cells were replated on collagen I in EGM-2 medium to generate ECs. These cells are shown at passage 5. FLK1-positive cells display typical "spindle" (early EPC) and "cobblestone-" (late EPC) like morphology in culture. (E) Flow cytometric analysis of differentiation of hESC- and hiPSC-derived FLK1-positive cells after sorting at passage 5 during differentiation into ECs in EGM-2 medium. (F) Immunofluorescence staining of hESC-ECs and hiPSC-ECs showed expression of CD31 and DiI-ac-LDL uptake in hiPSC-ECs. Similar images were observed from hESC-ECs (DiI-ac-LDL uptake in hESC-ECs is not shown). Nuclear counterstaining was performed with DAPI (blue). (G) Phase-contrast microscopic analysis showed that, similar to HUVECs, hESC-ECs and hiPSC-ECs after plating on Matrigel formed capillary-like structures after 14–21 days of differentiation. Data are presented as mean ± SD.

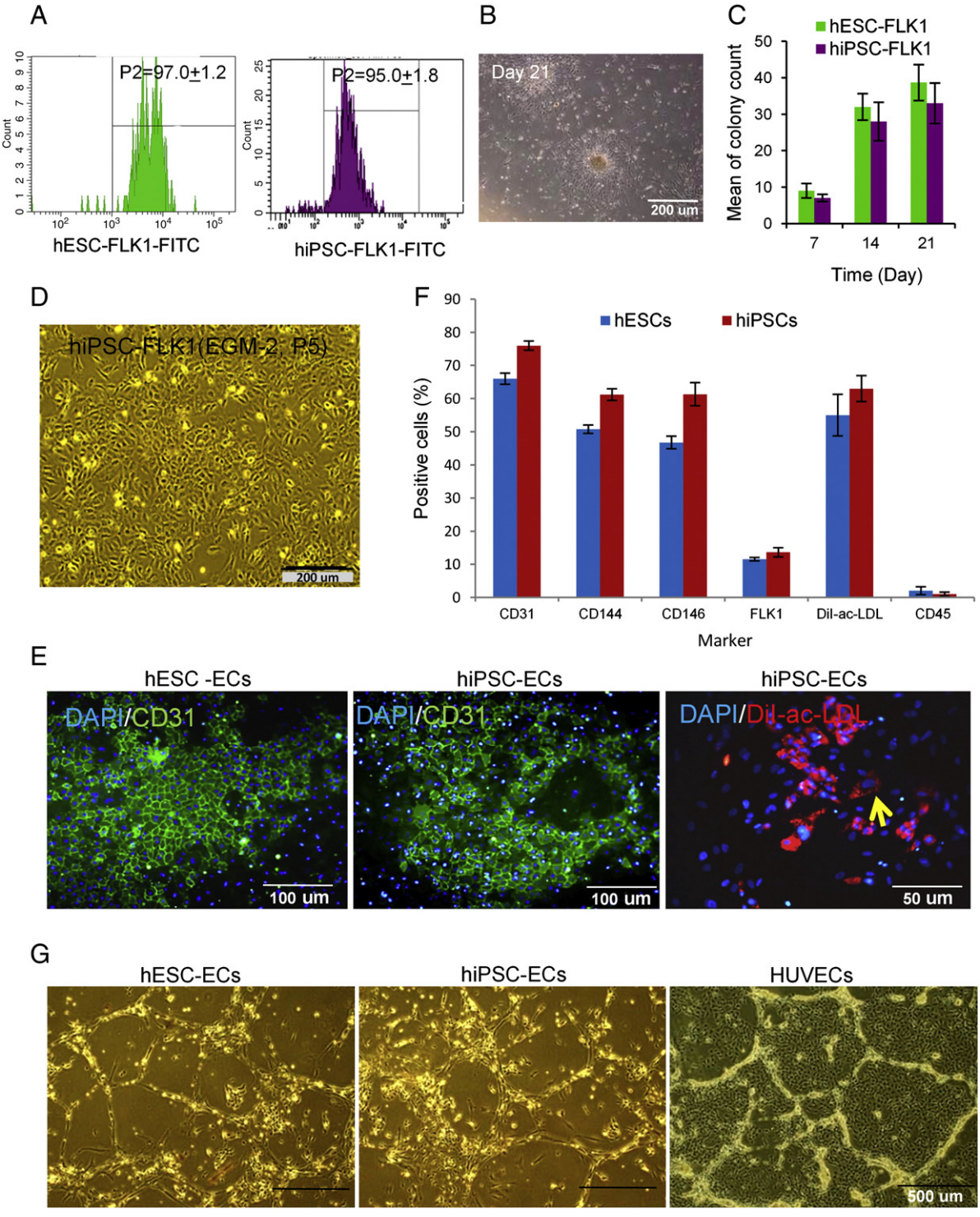
10×, and 100×. A total of 7–8 mice per group and 5–6 slides per mouse were used for counting total mast and degranulated cells.

Enzyme-linked immunosorbent assay of serum cytokine

Sera were obtained by cardiac puncture at two and four weeks of treatment with bleomycin (n = 6) and from transplanted mice at four weeks after transplantation (n = 7). Sera were stored at −80 °C. Serum levels of TGF-β1 were assed using an enzyme-linked immunosorbent assay (ELISA) kit (R&D System).

Statistical analysis

We used one-way ANOVA to compare the differences between independent groups as well as Levene's test for homogeneity of variance and the Kolmogorov–Smirnov for test of normality.



Two-way analysis of variance (ANOVA) was used to consider the simultaneous effect of two variables on outcome and the Kruskal–Wallis test compared the differences between independent groups' samples. We used repeated measures ANOVA followed by the Tukey post hoc test. Multiple group comparison was used to analyze group differences of the resultant data. Data were expressed as mean ± SD. $P \leq 0.05$ was considered significant.

Results

Differentiation of hESCs and hiPSCs to ECs

The experimental scheme for hESCs and hiPSCs differentiation into ECs (CD31-positive cells) and their transplantation used in this study is illustrated in Fig. 1A. Initially, the undifferentiated hESCs and hiPSCs were maintained in feeder-free conditions on Matrigel with DMEM-F12 medium. To induce differentiation, hESCs and hiPSCs were replated as small clusters on collagen IV-coated dishes in α-MEM medium and 10% FBS. Under these conditions, outgrown cells gradually changed their morphology from a circular mode into spindle and subsequently cobblestone mode in EGM-2 medium (Fig. 1B). Temporal expression of the EPC marker (FLK1) (Yamashita et al., 2000) of differentiating cells by flow cytometry showed that the proportion of FLK1-positive cells peaked at day 5 of differentiation after culturing on collagen IV-coated plates and in differentiation medium (Fig. 1C).

FLK1-positive cells were sorted by FACS on day 5 of differentiation and enriched to ~95% (Fig. 2A). The sorted FLK1-positive cells had colony forming potential in EndoCult medium (Fig. 2B). EC colonies appeared from 7 days after plating with the maximum colony count observed on day 21 (Fig. 2C). There was no significant difference between both cell lines in colony counts on the same days after plating.

The sorted FLK1-positive cells were replated on a collagen I-coated dish in endothelial growth medium (EGM2 medium in the presence of its supplements). These FLK1-positive sorted cells were successfully propagated for five passages with the use of 0.025%–0.01% trypsin–EDTA every 7–10 days on collagen I-coated dishes. These differentiated hESC-ECs and hiPSC-ECs from sorted FLK1-positive cells formed a "cobblestone" monolayer (Fig. 2D), and immunofluorescence staining revealed that these cells were positive for endothelial marker, CD31 (PECAM1; Fig. 2E). Flow cytometric analyses showed that differentiated hESC-ECs and hiPSC-ECs expressed endothelial

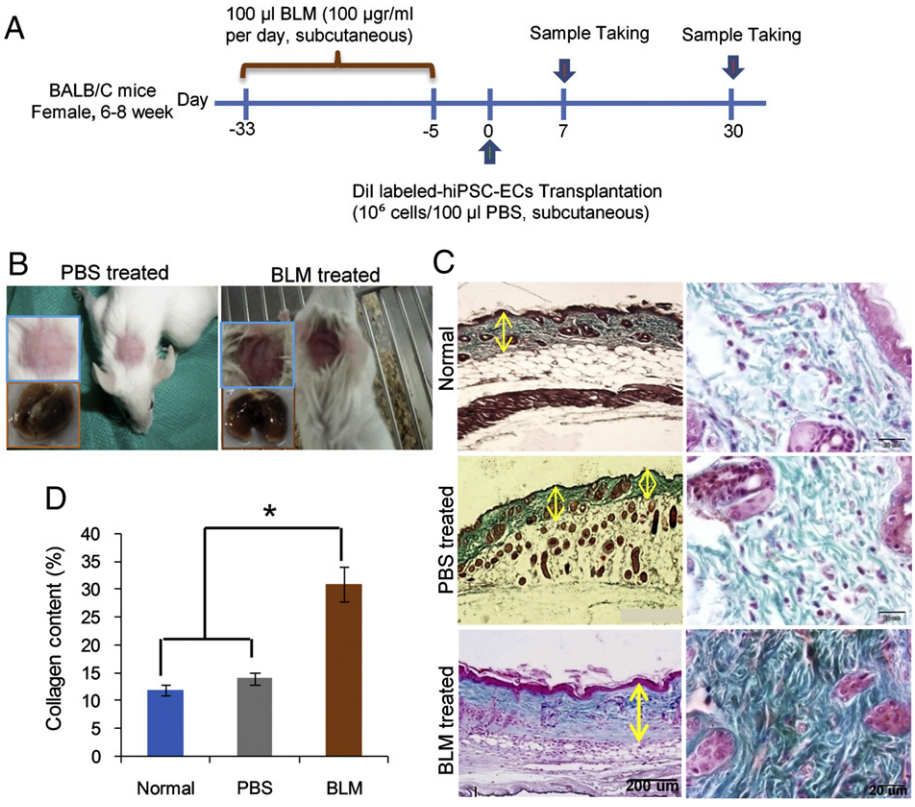


Figure 3 Histopathology of dermal sclerosis in mice. (A) Schematic illustration outlining the in vivo procedure comprising the study period, time of injury, and transplantation in the scleroderma (SSc) mouse model by bleomycin administration. (B) The SSc model. The gated pictures show the skin and lung of PBS- and BLM-treated mice. (C) Masson's trichrome (MT)-stained in normal, PBS- and bleomycin-treated skin. Marked dermal scleroses with thickened and homogenous collagen bundles (right panel) were induced. Arrows indicate increasing collagen amount and extension of the dermis. (D) Quantification of collagen content in normal, PBS- and bleomycin-treated mice skin. Dermal thickness increased after bleomycin injection, but PBS-treated mice did not exhibit an increase in dermal thickness. Significant differences were between bleomycin-treated mice with normal and PBS-treated mice (*$P<0.05$).

markers CD31 (68% and 75%), CD144 (50% and 61%) and CD146 (46% and 61%), respectively (Fig. 2F). EPC marker (FLK1) was down-regulated to ~11%–13% in the derived ECs. The cells were monocyte marker CD45 negative (1%–2%; Fig. 2F).

Uptake of DiI-ac-LDL has been used to characterize ECs (Voyta et al., 1984) and results showed that these differentiated cells were able to incorporate DiI-ac-LDL (55% in hESC-ECs and 63% in hiPSC-ECs), when cells were incubated with this substance (Figs. 2E and F). In addition, when hESC-ECs and hiPSC-ECs were plated on Matrigel, they formed tube-like structures after 14–21 days (Fig. 2G).

Induction of SSc animal model and transplantation of hiPSC-ECs

We induced an SSc animal model by subcutaneous local injection of bleomycin (Yamamoto, 2010) in BALB/C mice (Figs. 3A and B). MT staining demonstrated intense deposition

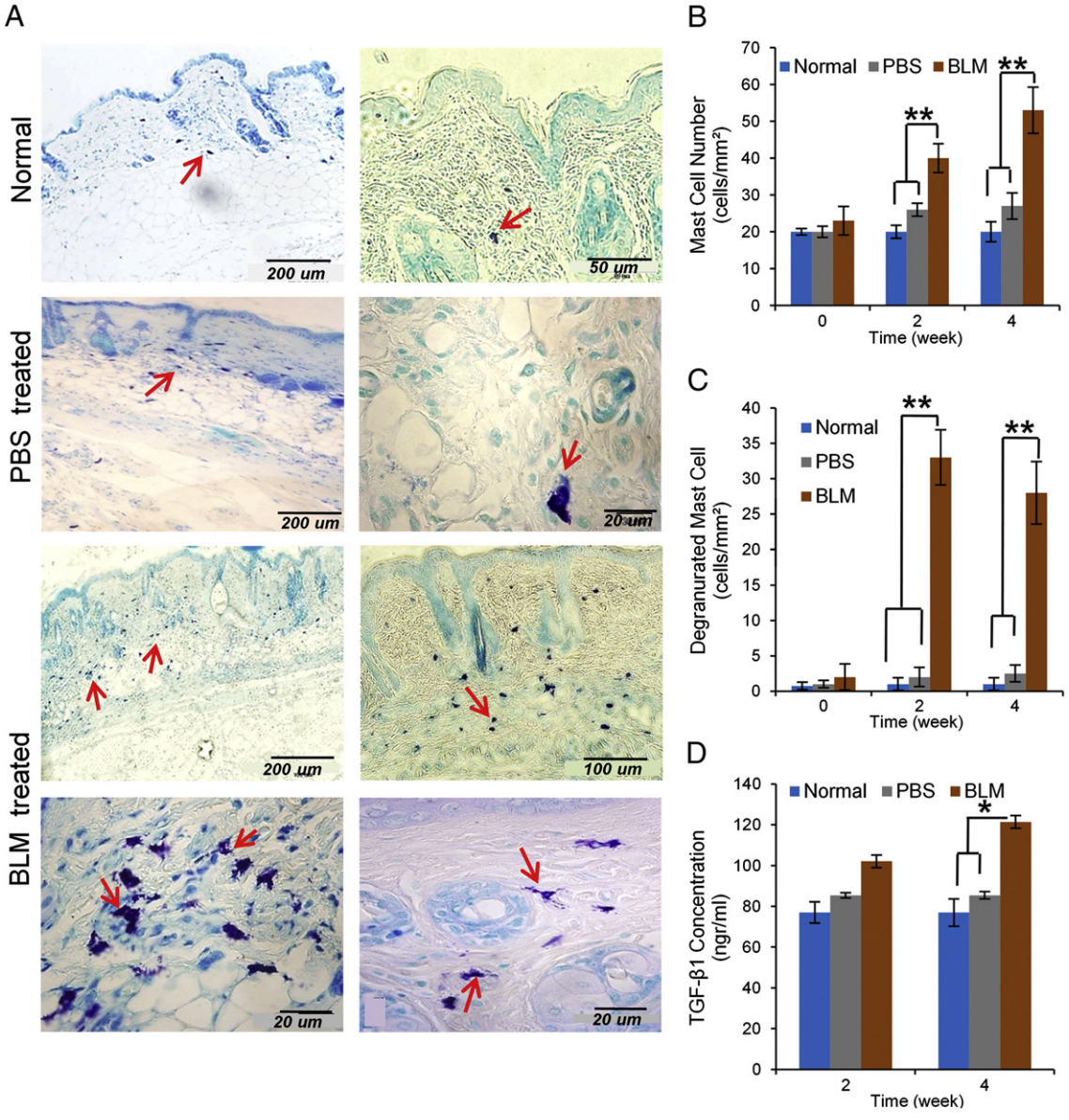


Figure 4 Characterization of bleomycin-induced scleroderma mouse model. (A) Mast cell infiltrates were prominent in the skin at 4 weeks of bleomycin treatment. Normal; PBS-treated; and bleomycin-treated skin in mice. Metachromasy phenomenon was shown in sclerotic skin by toluidine blue staining at 4 weeks. Right panel shows higher magnification. (B) The number of total and (C) degranulated mast cells was quantified by identification of toluidine blue staining at weeks 1, 2, and 4 (mean ± SD). Total number and degranulated mast cells show significant differences in bleomycin-treated mice in contrast to PBS-treated and normal mice (**$P<0.01$). There were no significant differences between PBS-treated and normal mice. (D) Serum TGF-β1 was measured by ELISA the day after application of bleomycin and PBS after the final application at weeks 2 and 4. Compared with PBS-treated or normal untreated mice, bleomycin-treated mice show a significant increase in TGF-β1 during weeks 2 and 4 ($P<0.05$).

of type 1 collagen in the dermis after bleomycin treatment when compared with PBS-treated mice (Fig. 3C). Cutaneous fibrosis was also quantified by analysis of collagen content. Results showed that collagen content in the punch-biopsied skins increased up to three-fold by bleomycin treatment compared to those treated with PBS (Fig. 3D).

As observed with toluidine blue staining, mast cells increased in numbers in parallel with the induction of SSc (Figs. 4A and B). Marked degranulation was noted, and compared with PBS-treated mice (Fig. 4C). Assessment with ELISA showed that the TGF-β1 serum level in bleomycin-treated mice was significantly higher than those of PBS-treated mice (Fig. 4D).

Before transplantation, hiPSC-ECs were sorted for the CD31 marker. After sorting, flow cytometry analyses showed that ~95% of the cells were CD31-positive (Fig. 5A). These cells expressed high levels of vWF (83%) and had rapid uptake of DiI-ac-LDL (93%; Figs. 5A and B). The cells also formed an in vitro "cobblestone" monolayer on a collagen I-coated dish (Fig. 5C). hESC-ECs also exhibited similar results after sorting

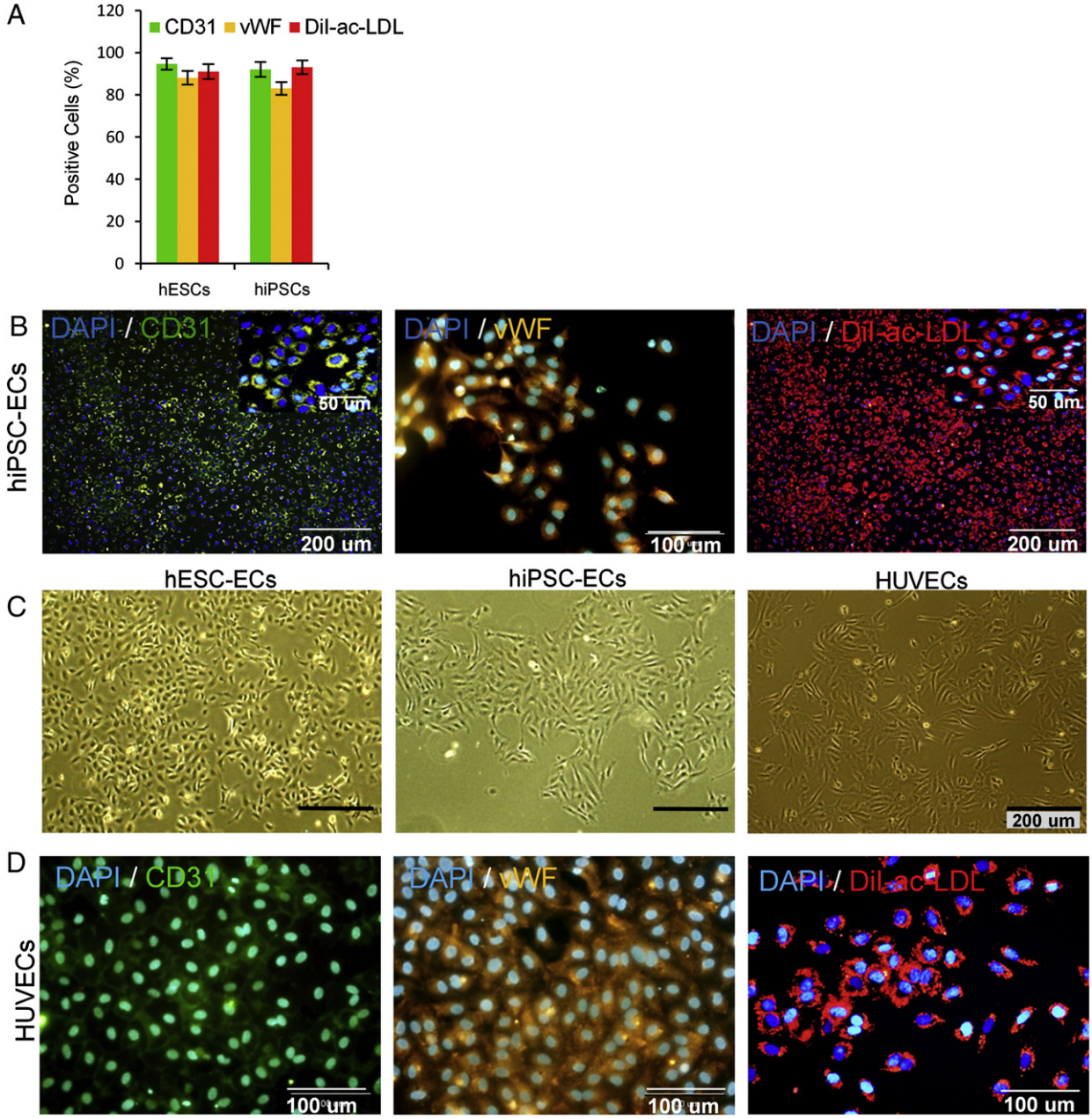


Figure 5 Isolation and expansion of hiPSC-ECs. (A) The quantification of CD31, vWF expression, and DiI-ac-LDL uptake in hESCs and hiPSCs-derived endothelial cells (ECs) after sorting using CD31 antibody. There were no significant differences between the two cell lines at the same experiments. (B) Fluorescence microscopy images from CD31, vWF expression, and DiI-ac-LDL uptake in hiPSC-ECs. The red color in the cytoplasm represents DiI-ac-LDL. (C) Phase-contrast microscopic analysis of recultured CD31-positive sorted cells on a collagen I-coated dish. (D) Isolated human umbilical vein ECs (HUVECs) were used as the positive control.

(Fig. 5). Isolated human umbilical vein ECs (HUVECs) were used as the positive control (Fig. 5D).

Next, we transplanted CD31-purified positive cells that were derived from hiPSCs into the mice model. For tracing transplanted cells, we used DiI labeling. According to fluorescence microscopy images one week after transplantation, DiI-labeled hiPSC-ECs localized robustly at the injection site of the skin (Fig. 6A). However, four weeks after transplantation these labeled cells were distributed in skin tissue along with cell division (data not shown) and homed around vessels, particularly the distracted micro vessels (Fig. 6A). These DiI-positive cells were positive for human vWF antigen (Fig. 6C).

Quantitative analysis of MT staining of tissue sections, one and four weeks post-transplantation, showed significant reduction in collagen deposition in the hiPSC-EC transplanted group four weeks post-transplantation compared to the control group (Fig. 7).

There were decreased counts in the numbers of total and degranulated mast cells four weeks post-transplantation (Figs. 8A–C), but the serum levels of TGF-β1 did not significantly change after cell transplantation when compared with the control group (Fig. 8D).

Discussion

Endothelium destruction and loss of ECs are the main events in SSc patients. To date, few cell therapy studies have been performed for SSc.

In this study, we described the differentiation of hiPSCs into efficient functional ECs and compared them with hESC-ECs. We have found that hiPSCs, similar to hESCs, can be differentiated into ECs by the use of a sequential combination of FLK1-positive (EPC marker) and CD31-positive (late EC marker) sorting. These ECs show typical endothelial cobblestone morphology, express lineage specific markers (CD31, CD144, and CD146), and can take up DiI-ac-LDL as well as form endothelial tubes on Matrigel. These results are in agreement with other recent reports on the differentiation and functionality of ESC and iPSC-derived ECs (Kaufman et al., 2004; Kim and von Recum, 2009; Levenberg et al., 2002; Li et al., 2007, 2011; Rufaihah et al., 2011; Sone et al., 2003; Yamashita et al., 2000).

We induced SSc in a mouse model by administering daily subcutaneous injections of bleomycin. The model was characterized by accumulation of collagen bundles, increased mast cell numbers (particularly in the edematous phase), observation of degranulated mast cells, and the release of TGF-β1 as previously noted (Jinnin et al., 2004; Li et al., 2007; Reinecke and Murry, 2002; Yamamoto, 2010). We observed that transplanted hiPSC-ECs showed homing around damaged vessels, with improvements in collagen deposition, the numbers of total and degranulated mast cells, in addition to superficial injury healing four weeks post-transplantation. The beneficial effects of hESC-ECs and hiPSC-ECs in the setting of myocardial or limb ischemia have also been reported (James et al., 2010; Kane et al., 2010; Levenberg et al., 2002, 2010; Li et al., 2009; Nourse et al., 2010; Rufaihah et al., 2010; Sone et al., 2007).

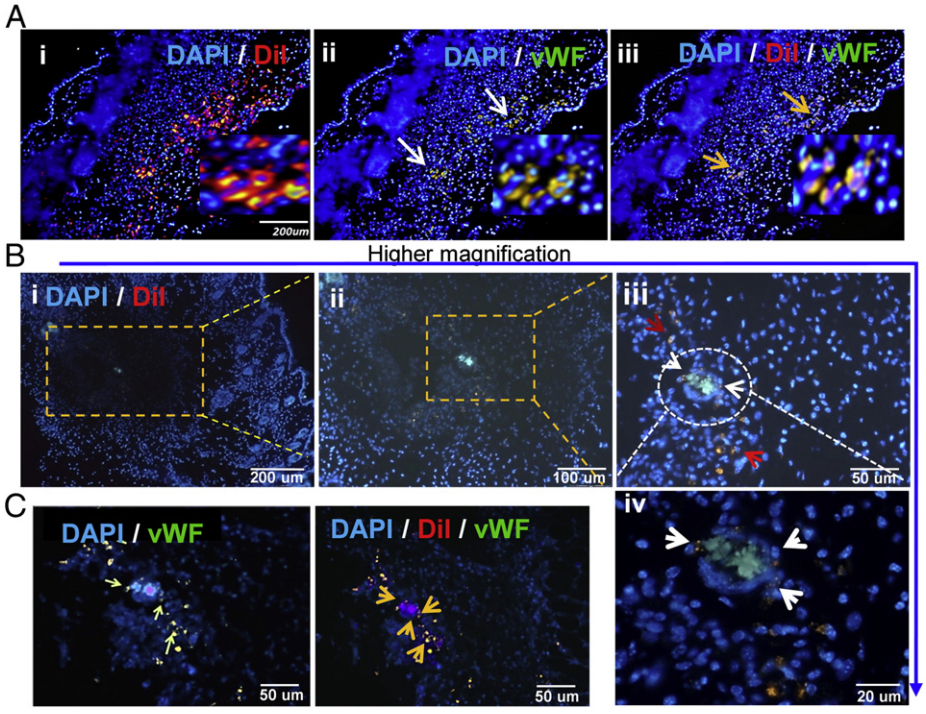


Figure 6 Transplantation of DiI-labeled hiPSC-ECs into the scleroderma (SSc) mouse model. DiI-labeled hiPSC-ECs (1×10^6/100 μl EGM-2) were subcutaneously transplanted into bleomycin-induced dorsal neck skin. (A) Assessment of labeled cells homing one week after transplantation shows that: (i) hiPSC-ECs are present in skin tissue; (ii) labeled cells are positive for human vWF antigen; and (iii) the merge of DiI and vWF-positive cells. (B) (i) hiPSC-ECs in skin tissue four weeks after transplantation. (ii), (iii) and (iv) show DiI-labeled hiPSC-ECs around micro vessels. The magnification was increased from (i) to (iv). (C) Homed cells positive for human vWF antigen after four weeks. Merge of DiI and vWF-positive cells is shown.

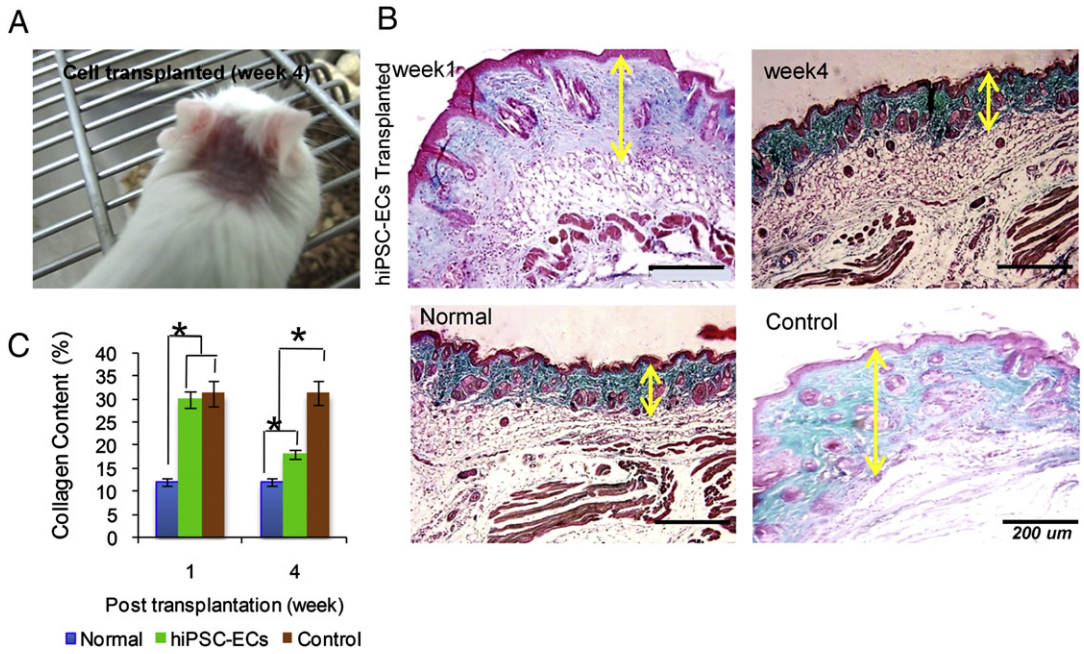


Figure 7 Photomicrographs of scleroderma mouse skin sections after hiPSC-EC transplantation. (A) hiPSC-EC transplanted mouse four weeks after transplantation showed improvement. (B) hiPSC-EC transplanted mice, one week after transplantation showed packed collagen fibers that extended from the epidermis to the underside muscle layer. The sections were stained with MT. Transplanted hiPSC-EC group four weeks after transplantation showed decreased collagen content. Normal and control groups four weeks after final bleomycin treatment. (C) Quantification of collagen content after transplantation. Collagen content one week after transplantation in hiPSC-ECs and control groups shows significant difference with normal mice, whereas four weeks after transplantation the hiPSC-EC group shows significant decreases in collagen content in contrast to the control group. (Both control and hiPSC-EC groups were treated with bleomycin before transplantation. The control group was only injected with EGM2 medium on the transplantation day. *$P<0.05$.)

The mechanism for this improvement remains to be determined; however, it may be based on the following: (i) attendance of a subpopulation of mature or precursor cells that survive, migrate, and differentiate to ECs, (ii) paracrine effects, and/or (iii) the prevention of mononuclear cell infiltration, thus resulting in improvement of symptoms (Fig. 9). We have observed the incorporation of hiPSC-ECs into existing damaged vasculature.

Poor donor cell survival of transplanted hiPSC-ECs has been reported in other studies as indicated by serial histology, the Taqman Sry PCR technique, or TUNEL apoptosis assay (Li et al., 2007; Reinecke and Murry, 2002). This may be related to stimulation of the immune system of animals by human cells or may be related to inappropriate receipt of a signal required for efficient integration of hiPSC-ECs into mouse vasculature. Alternatively, it is likely that the injected cells have a paracrine effect. Recently, it has been demonstrated that transplanted hiPSC-ECs in an ischemic limb model caused secretion of the angiogenic cytokines and growth factors, including angiopoietin-1, vascular endothelial growth factor-A and -C, and platelet-derived growth factor-AA (Rufaihah et al., 2011). However, additional studies are necessary to test our hypothesis. In addition, the perivascular infiltration of mononuclear cells (MNC) is associated with increased collagen synthesis in adjacent fibroblasts (Jinnin et al., 2004). Therefore hiPSC-EC transplantation, homing, and incorporation in the reconstruction of damaged vascular barriers can prevent MSC infiltration, which will lead to the prevention of extra collagen synthesis and subsequent occurrence of fibrosis by intervening in the fibrotic process.

No evidence of tumor formation has been demonstrated in the transplanted group. Therefore, although teratomas are predominantly derived from the hiPSC graft, purified pluripotent stem cell-ECs provide an opportunity for cell therapy.

One of the limitations of our study is that we focused on one hiPSC line; additional research on more hiPSC lines is necessary. According to our results, as proven by previous studies, there is a limitation in the expansion potential of hiPSC-ECs when compared with hESC-ECs (Li et al., 2011). Another limitation is cell labeling with DiI, and the use of immunosuppressed mice which require more reliable cell tracking, noninvasive cell tracking, and immunodeficient mice. Furthermore, although autologous hiPSCs minimize (Zhao et al., 2011) or possibly eliminate the need for immune suppression after cell transplantation, however a number of technical issues such as 'epigenetic memory' and karyotypic instability during culture (Ji et al., 2010; Kim et al., 2010; Lister et al., 2011; Marchetto et al., 2009; Polo et al., 2010) need to be addressed before they are considered for clinical applications. Some key advances aimed at overcoming these safety concerns have been reached with the production of iPS

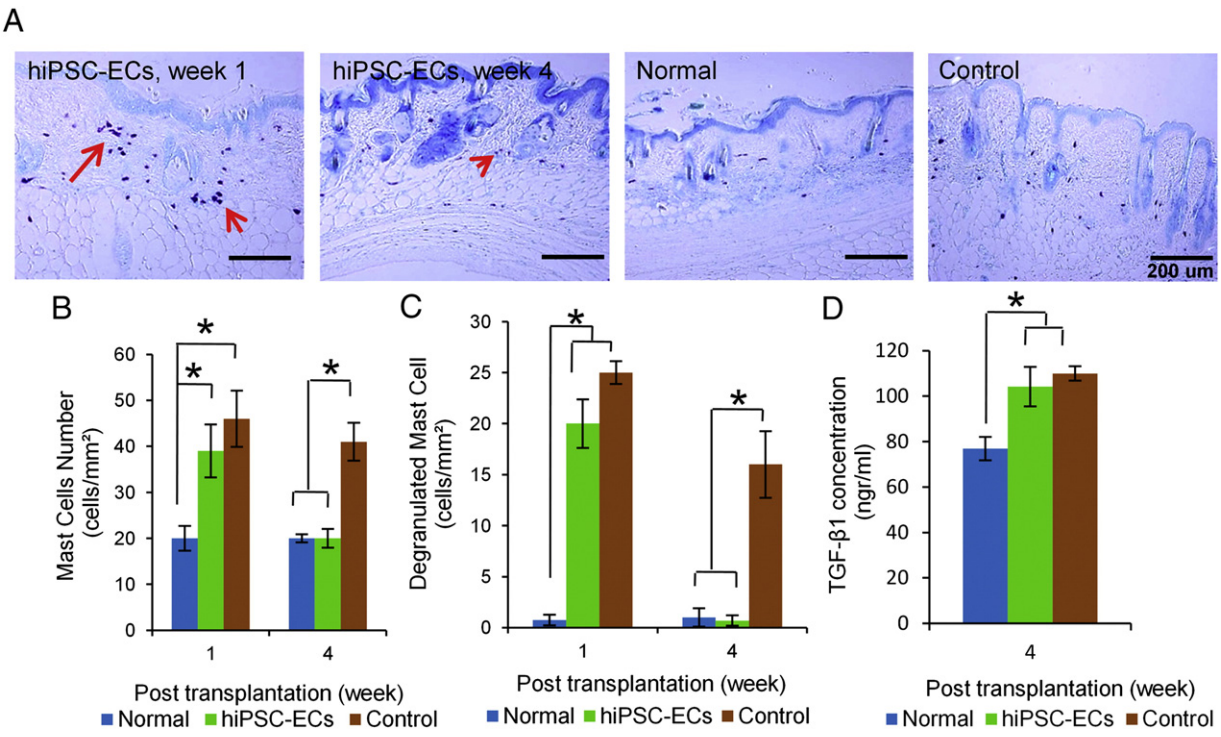


Figure 8 Assessment of mast cell numbers and serum TGF-β1 after hiPSC-EC transplantation. (A) Metachromasy phenomenon was shown by toluidine blue staining. The control group received bleomycin for 4 weeks and PBS (or EGM-2 without cells) only on the transplantation day. (B) Total mast cell and (C) degranulated mast cell number. Four weeks after transplantation, total and degranulated mast cell numbers in the hiPSC-EC group reached the normal range. (D) Upregulation in serum TGF-β1 four weeks after transplantation was observed in both control and cell transplanted groups in comparison with normal ones. *$P<0.05$.

cells (for review see Gonzalez et al., 2011; Seifinejad et al., 2010; Stadtfeld and Hochedlinger, 2010).

In conjunction, these early data have shown proof of concept that transplantation of ECs derived from hiPSCs, similar to hESC-ESc, can provide some benefits in the setting for SSc regeneration. With further validation, the ECs that are isolated from hESCs and hiPSCs, as described here, can provide a continual endothelial cell source of therapy for vascular regeneration in SSc in addition to other diseases with endothelial abnormalities.

Acknowledgments

This study was funded by a grant provided by the Royan Institute. We thank Mr. Ehsan Janzamin for his unlimited assistance in the Flow Cytometry Laboratory, Dr. Abass

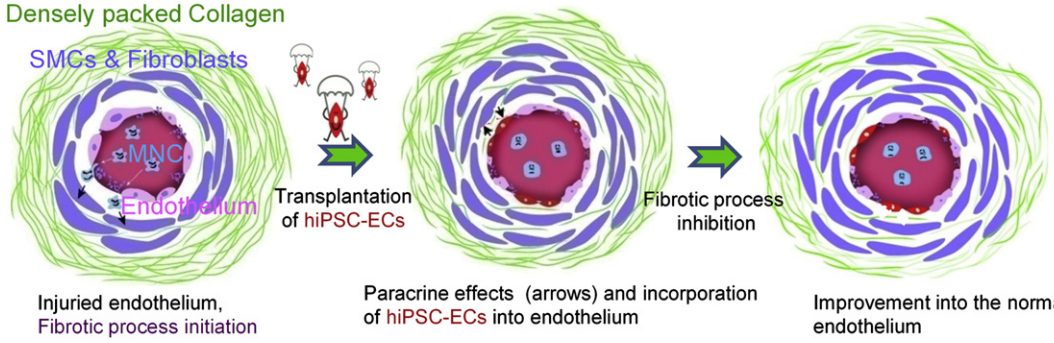


Figure 9 A possible mechanism for scleroderma improvement by hiPSC-EC transplantation. By incorporation of the transplanted cells into the existing damaged vasculature or by a paracrine effect and/or prevention of perivascular infiltration of mononuclear cells (MNCs) we could improve collagen deposition, reduce the number of total and degranulated mast cells, and improve injury in a mouse model of SSc.

Piryaei and Leila Sattarian in the Histology Laboratory, Mr. Chehrazi for statistical analysis, and Miss Saloomeh Gooyan for schematic illustration.

References

Asahara, T., Masuda, H., Takahashi, T., Kalka, C., Pastore, C., Silver, M., Kearne, M., Magner, M., Isner, J.M., 1999. Bone marrow origin of endothelial progenitor cells responsible for postnatal vasculogenesis in physiological and pathological neovascularization. Circ. Res. 85, 221–228.

Baharvand, H., Ashtiani, S.K., Taee, A., Massumi, M., Valojerdi, M.R., Yazdi, P.E., Moradi, S.Z., Farrokhi, A., 2006. Generation of new human embryonic stem cell lines with diploid and triploid karyotypes. Develop. Growth Differ. 48, 117–128.

Balconi, G., Spagnuolo, R., Dejana, E., 2000. Development of endothelial cell lines from embryonic stem cells: a tool for studying genetically manipulated endothelial cells in vitro. Arterioscler. Thromb. Vasc. Biol. 20, 1443–1451.

Cipriani, P., Guiducci, S., Miniati, I., Cinelli, M., Urbani, S., Marrelli, A., Dolo, V., Pavan, A., Saccardi, R., Tyndall, A., Giacomelli, R., Cerinic, M.M., 2007. Impairment of endothelial cell differentiation from bone marrow-derived mesenchymal stem cells: new insight into the pathogenesis of systemic sclerosis. Arthritis Rheum. 56, 1994–2004.

Fleming, J.N., Nash, R.A., McLeod, D.O., Fiorentino, D.F., Shulman, H.M., Connolly, M.K., Molitor, J.A., Henstorf, G., Lafyatis, R., Pritchard, D.K., Adams, L.D., Furst, D.E., Schwartz, S.M., 2008. Capillary regeneration in scleroderma: stem cell therapy reverses phenotype? PLoS One 3, e1452.

Gabrielli, A., Avvedimento, E.V., Krieg, T., 2009. Scleroderma. N. Engl. J. Med. 360, 1989–2003.

Gonzalez, F., Boue, S., Belmonte, J.C., 2011. Methods for making induced pluripotent stem cells: reprogramming a la carte. Nat. Rev. Genet. 12, 231–242.

Heeschen, C., Lehmann, R., Honold, J., Assmus, B., Aicher, A., Walter, D.H., Martin, H., Zeiher, A.M., Dimmeler, S., 2004. Profoundly reduced neovascularization capacity of bone marrow mononuclear cells derived from patients with chronic ischemic heart disease. Circulation 109, 1615–1622.

Hill, J.M., Zalos, G., Halcox, J.P., Schenke, W.H., Waclawiw, M.A., Quyyumi, A.A., Finkel, T., 2003. Circulating endothelial progenitor cells, vascular function, and cardiovascular risk. N. Engl. J. Med. 348, 593–600.

Isner, J.M., Kalka, C., Kawamoto, A., Asahara, T., 2001. Bone marrow as a source of endothelial cells for natural and iatrogenic vascular repair. Ann. N. Y. Acad. Sci. 953, 75–84.

James, D., Nam, H.S., Seandel, M., Nolan, D., Janovitz, T., Tomishima, M., Studer, L., Lee, G., Lyden, D., Benezra, R., Zaninovic, N., Rosenwaks, Z., Rabbany, S.Y., Rafii, S., 2010. Expansion and maintenance of human embryonic stem cell-derived endothelial cells by TGFbeta inhibition is Id1 dependent. Nat. Biotechnol. 28, 161–166.

Ji, H., Ehrlich, L.I., Seita, J., Murakami, P., Doi, A., Lindau, P., Lee, H., Aryee, M.J., Irizarry, R.A., Kim, K., Rossi, D.J., Inlay, M.A., Serwold, T., Karsunky, H., Ho, L., Daley, G.Q., Weissman, I.L., Feinberg, A.P., 2010. Comprehensive methylome map of lineage commitment from haematopoietic progenitors. Nature 467, 338–342.

Jinnin, M., Ihn, H., Yamane, K., Tamaki, K., 2004. Interleukin-13 stimulates the transcription of the human alpha2(I) collagen gene in human dermal fibroblasts. J. Biol. Chem. 279, 41783–41791.

Kahaleh, B., 2008. Vascular disease in scleroderma: mechanisms of vascular injury. Rheum. Dis. Clin. N. Am. 34, 57–71 (vi).

Kane, N.M., Meloni, M., Spencer, H.L., Craig, M.A., Strehl, R., Milligan, G., Houslay, M.D., Mountford, J.C., Emanueli, C., Baker, A.H., 2010. Derivation of endothelial cells from human embryonic stem cells by directed differentiation: analysis of microRNA and angiogenesis in vitro and in vivo. Arterioscler. Thromb. Vasc. Biol. 30, 1389–1397.

Kaufman, D.S., Lewis, R.L., Hanson, E.T., Auerbach, R., Plendl, J., Thomson, J.A., 2004. Functional endothelial cells derived from rhesus monkey embryonic stem cells. Blood 103, 1325–1332.

Kim, S., von Recum, H.A., 2009. Endothelial progenitor populations in differentiating embryonic stem cells I: identification and differentiation kinetics. Tissue Eng. Part A 15, 3709–3718.

Kim, K., Doi, A., Wen, B., Ng, K., Zhao, R., Cahan, P., Kim, J., Aryee, M.J., Ji, H., Ehrlich, L.I., Yabuuchi, A., Takeuchi, A., Cunniff, K.C., Hongguang, H., McKinney-Freeman, S., Naveiras, O., Yoon, T.J., Irizarry, R.A., Jung, N., Seita, J., Hanna, J., Murakami, P., Jaenisch, R., Weissleder, R., Orkin, S.H., Weissman, I.L., Feinberg, A.P., Daley, G.Q., 2010. Epigenetic memory in induced pluripotent stem cells. Nature 467, 285–290.

Levenberg, S., Golub, J.S., Amit, M., Itskovitz-Eldor, J., Langer, R., 2002. Endothelial cells derived from human embryonic stem cells. Proc. Natl. Acad. Sci. U. S. A. 99, 4391–4396.

Levenberg, S., Ferreira, L.S., Chen-Konak, L., Kraehenbuehl, T.P., Langer, R., 2010. Isolation, differentiation and characterization of vascular cells derived from human embryonic stem cells. Nat. Protoc. 5, 1115–1126.

Li, Z., Wu, J.C., Sheikh, A.Y., Kraft, D., Cao, F., Xie, X., Patel, M., Gambhir, S.S., Robbins, R.C., Cooke, J.P., Wu, J.C., 2007. Differentiation, survival, and function of embryonic stem cell derived endothelial cells for ischemic heart disease. Circulation 116, I46–I54.

Li, Z., Wilson, K.D., Smith, B., Kraft, D.L., Jia, F., Huang, M., Xie, X., Robbins, R.C., Gambhir, S.S., Weissman, I.L., Wu, J.C., 2009. Functional and transcriptional characterization of human embryonic stem cell-derived endothelial cells for treatment of myocardial infarction. PLoS One 4, e8443.

Li, Z., Hu, S., Ghosh, Z., Han, Z., Wu, J.C., 2011. Functional characterization and expression profiling of human induced pluripotent stem cell- and embryonic stem cell-derived endothelial cells. Stem Cells Dev. 20, 1701–1710.

Lister, R., Pelizzola, M., Kida, Y.S., Hawkins, R.D., Nery, J.R., Hon, G., Antosiewicz-Bourget, J., O'Malley, R., Castanon, R., Klugman, S., Downes, M., Yu, R., Stewart, R., Ren, B., Thomson, J.A., Evans, R.M., Ecker, J.R., 2011. Hotspots of aberrant epigenomic reprogramming in human induced pluripotent stem cells. Nature 471, 68–73.

Marchetto, M.C., Yeo, G.W., Kainohana, O., Marsala, M., Gage, F.H., Muotri, A.R., 2009. Transcriptional signature and memory retention of human-induced pluripotent stem cells. PLoS One 4, e7076.

Nourse, M.B., Halpin, D.E., Scatena, M., Mortisen, D.J., Tulloch, N.L., Hauch, K.D., Torok-Storb, B., Ratner, B.D., Pabon, L., Murry, C.E., 2010. VEGF induces differentiation of functional endothelium from human embryonic stem cells: implications for tissue engineering. Arterioscler. Thromb. Vasc. Biol. 30, 80–89.

Polo, J.M., Liu, S., Figueroa, M.E., Kulalert, W., Eminli, S., Tan, K.Y., Apostolou, E., Stadtfeld, M., Li, Y., Shioda, T., Natesan, S., Wagers, A.J., Melnick, A., Evans, T., Hochedlinger, K., 2010. Cell type of origin influences the molecular and functional properties of mouse induced pluripotent stem cells. Nat. Biotechnol. 28, 848–855.

Reinecke, H., Murry, C.E., 2002. Taking the death toll after cardiomyocyte grafting: a reminder of the importance of quantitative biology. J. Mol. Cell. Cardiol. 34, 251–253.

Rufaihah, A.J., Haider, H.K., Heng, B.C., Ye, L., Tan, R.S., Toh, W.S., Tian, X.F., Sim, E.K., Cao, T., 2010. Therapeutic angiogenesis by transplantation of human embryonic stem cell-derived $CD133^{+}$ endothelial progenitor cells for cardiac repair. Regen. Med. 5, 231–244.

Rufaihah, A.J., Huang, N.F., Jame, S., Lee, J.C., Nguyen, H.N., Byers, B., De, A., Okogbaa, J., Rollins, M., Reijo-Pera, R.,

Gambhir, S.S., Cooke, J.P., 2011. Endothelial cells derived from human iPSCS increase capillary density and improve perfusion in a mouse model of peripheral arterial disease. Arterioscler. Thromb. Vasc. Biol. 31, e72–e79.

Seifinejad, A., Tabebordbar, M., Baharvand, H., Boyer, L.A., Salekdeh, G.H., 2010. Progress and promise towards safe induced pluripotent stem cells for therapy. Stem Cell Rev. 6, 297–306.

Sone, M., Itoh, H., Yamashita, J., Yurugi-Kobayashi, T., Suzuki, Y., Kondo, Y., Nonoguchi, A., Sawada, N., Yamahara, K., Miyashita, K., Park, K., Shibuya, M., Nito, S., Nishikawa, S., Nakao, K., 2003. Different differentiation kinetics of vascular progenitor cells in primate and mouse embryonic stem cells. Circulation 107, 2085–2088.

Sone, M., Itoh, H., Yamahara, K., Yamashita, J.K., Yurugi-Kobayashi, T., Nonoguchi, A., Suzuki, Y., Chao, T.H., Sawada, N., Fukunaga, Y., Miyashita, K., Park, K., Oyamada, N., Sawada, N., Taura, D., Tamura, N., Kondo, Y., Nito, S., Suemori, H., Nakatsuji, N., Nishikawa, S., Nakao, K., 2007. Pathway for differentiation of human embryonic stem cells to vascular cell components and their potential for vascular regeneration. Arterioscler. Thromb. Vasc. Biol. 27, 2127–2134.

Stadtfeld, M., Hochedlinger, K., 2010. Induced pluripotency: history, mechanisms, and applications. Genes Dev. 24, 2239–2263.

Takahashi, K., Tanabe, K., Ohnuki, M., Narita, M., Ichisaka, T., Tomoda, K., Yamanaka, S., 2007. Induction of pluripotent stem cells from adult human fibroblasts by defined factors. Cell 131, 861–872.

Thomson, J.A., Itskovitz-Eldor, J., Shapiro, S.S., Waknitz, M.A., Swiergiel, J.J., Marshall, V.S., Jones, J.M., 1998. Embryonic stem cell lines derived from human blastocysts. Science 282, 1145–1147.

Totonchi, M., Taei, A., Seifinejad, A., Tabebordbar, M., Rassouli, H., Farrokhi, A., Gourabi, H., Aghdami, N., Hosseini-Salekdeh, G., Baharvand, H., 2010. Feeder- and serum-free establishment and expansion of human induced pluripotent stem cells. Int. J. Dev. Biol. 54, 877–886.

Trojanowska, M., 2010. Cellular and molecular aspects of vascular dysfunction in systemic sclerosis. Nat. Rev. Rheumatol. 6, 453–460.

Vasa, M., Fichtlscherer, S., Aicher, A., Adler, K., Urbich, C., Martin, H., Zeiher, A.M., Dimmeler, S., 2001. Number and migratory activity of circulating endothelial progenitor cells inversely correlate with risk factors for coronary artery disease. Circ. Res. 89, E1–E7.

Voyta, J.C., Via, D.P., Butterfield, C.E., Zetter, B.R., 1984. Identification and isolation of endothelial cells based on their increased uptake of acetylated-low density lipoprotein. J. Cell Biol. 99, 2034–2040.

Yamamoto, T., 2009. Scleroderma—pathophysiology. Eur. J. Dermatol. 19, 14–24.

Yamamoto, T., 2010. Animal model of systemic sclerosis. J. Dermatol. 37, 26–41.

Yamashita, J., Itoh, H., Hirashima, M., Ogawa, M., Nishikawa, S., Yurugi, T., Naito, M., Nakao, K., Nishikawa, S., 2000. Flk1-positive cells derived from embryonic stem cells serve as vascular progenitors. Nature 408, 92–96.

Yu, J., Vodyanik, M.A., Smuga-Otto, K., Antosiewicz-Bourget, J., Frane, J.L., Tian, S., Nie, J., Jonsdottir, G.A., Ruotti, V., Stewart, R., Thomson, J.A., 2007. Induced pluripotent stem cell lines derived from human somatic cells. Science 318, 1917–1920.

Zhao, T., Zhang, Z.N., Rong, Z., Xu, Y., 2011. Immunogenicity of induced pluripotent stem cells. Nature 474, 212–215.